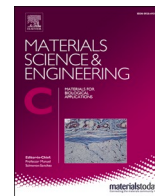




Contents lists available at ScienceDirect

## Materials Science &amp; Engineering C

journal homepage: [www.elsevier.com/locate/msec](http://www.elsevier.com/locate/msec)Cracks in consolidants containing TiO<sub>2</sub> as a habitat for biological colonization: A case of quaternary bioreceptivityP. Sanmartín<sup>a,\*</sup>, D. Noya-Pintos<sup>b</sup>, E. Fuentes<sup>a</sup>, J.S. Pozo-Antonio<sup>c</sup><sup>a</sup> Departamento de Edafología e Química Agrícola, Facultade de Farmacia, Universidade de Santiago de Compostela, 15782 Santiago de Compostela, Spain<sup>b</sup> Escola Superior de Conservación e Restauración de Bens Culturais de Galicia, 36002 Pontevedra, Spain<sup>c</sup> CINTECX, GESSMin Group, Departamento de Enxeñaría dos Recursos Naturais e Medio Ambiente, Escola de Enxeñaría de Minas e Enerxía, University of Vigo, Vigo 36310, Spain

## ARTICLE INFO

## Keywords:

Biodeterioration  
Greening  
Consolidant  
Stone  
Nanotechnology  
TiO<sub>2</sub>

## ABSTRACT

The recently proposed concept of quaternary bioreceptivity applies to substrates treated with coating materials and it is considered in the present study with the alga *Bracteacoccus minor* and the cyanobacterium *Nostoc* sp. onto granite specimens treated with ethyl silicate and nano-sized silica doped with different amounts of TiO<sub>2</sub> (0, 0.5, 1 and 3 wt%). The findings showed a lack of correlation between the amount of TiO<sub>2</sub> and the level of colonization (main bioreceptivity estimator) to the presence of cracks on the surface, which annul the biocidal power of TiO<sub>2</sub>. Crack formation, which depends on the mechanical properties, greatly influences the bioreceptivity of the material. Thus, the cracks provided anchor points where water is retained, in turn strongly influencing the early stages of colonization kinetics, to a greater extent than the biocidal power of TiO<sub>2</sub>, which will probably increase as the biofilm develops over the entire surface. In addition, although the cracks were more abundant and wider in the ethyl silicate-based consolidant, the nano-sized silica provided better anchoring points, making the material treated with the corresponding consolidant more bioreceptive.

## 1. Introduction

Bioreceptivity, defined by Guillitte as “the ability of a material to be colonized by living organisms”, can be primary “when the properties of the material remain very similar or identical to those of its initial state”, secondary “when characteristics of these properties evolve over time under the action of colonizing organisms or other factors causing change”, or tertiary “when any human activity affecting the material occurs - consolidation, coating with a biocide or surface polishing -” [1]. It has recently been suggested that the term tertiary bioreceptivity as defined by Guillitte [1] should be used to refer to cleaned material (including when surface roughness is altered by laser-based or other cleaning treatments) and that the term ‘quaternary bioreceptivity’ should be used to refer to those cases in which new materials that can leave residues, such as coatings or chemical products, are added to the original material [2]. This proposal is strongly supported by the findings of previous studies [e.g., [3–9]] that demonstrate the changes in the colonizing behavior of populations of autotrophic and heterotrophic microorganisms (mainly fungi) when new components (such as plastic-based consolidants or chemical biocides) are added to restoration

treatments.

The chemical composition of the material added via treatments can support microbial growth. Caneva and Nugari [[4], *apud* [10]] observed that the use of a consolidant made from mucilaginous carbohydrate-like extracts from a local plant (*Escobilla*) growing at the Mayan site of Joya de Ceren (El Salvador) favoured growth of fungi, particularly of actinomycetes. In the Catacombs of Domitilla (Rome, Italy), a biocidal treatment composed by quaternary ammonium compounds and octylisothiazolone triggered the proliferation of bacteria with high hydrolytic enzymatic activity [8]. In Campeche (Mexico), restored mortars containing fatty acids promoted early endolithic phototrophic colonization by cyanobacteria and bryophytes on the facade of the San Roque church [11].

Fungi can cause physical disruption of the coating surface, resulting in biopitting and formation of cracks and fissures, where fungal growth can occur. This phenomenon has been observed on the surface of stony materials such as marble and other calcareous rocks such as limestones [12,13] and on the surface of acrylic resins on the marble-built Tempio Malatestiano (Rimini, Italy) [14] and Milan cathedral (Milan, Italy) [6,7]. Furthermore, and relevant to the present study, cracking not only

\* Corresponding author.

E-mail address: [patricia.sanmartin@usc.es](mailto:patricia.sanmartin@usc.es) (P. Sanmartín).<https://doi.org/10.1016/j.msec.2021.112058>

Received 9 February 2021; Received in revised form 15 March 2021; Accepted 20 March 2021

Available online 25 March 2021

0928-4931/© 2021 The Authors. Published by Elsevier B.V. This is an open access article under the CC BY license (<http://creativecommons.org/licenses/by/4.0/>).

occur in coatings as a result of the effect of biodeteriogens, but can also occur immediately after application of the product, due to the high capillary pressures supported by the gel network during drying, especially in micropores typical of silicon-based stone consolidants like tetraethyl-ortho-silicate [15–19]. The same has also been observed in consolidants to which TiO<sub>2</sub> has been added, with greater amounts of TiO<sub>2</sub> increasing the risk of micro-cracks occurring in the coating [20]. The cracks in the coating modify the surface, altering the roughness and surface porosity; both parameters have been shown to play a key role in the bioreceptivity of substrates to microalgae and cyanobacteria [21,22]. Both autotrophs are considered early colonizers of stone building materials, along with ubiquitous bacteria [23,10].

Microalgae and cyanobacteria are the main organisms that have been used as models in bioreceptivity studies [24–28]. The bioreceptivity of material to microalgae and cyanobacteria can be assessed under laboratory conditions in the following ways: (1) by inoculating the target material with the live microorganisms; (2) by maintaining the material under accelerated growth conditions until the growth or biofilm maturity are stable or until a certain point is reached in the experiment; and (3) by quantifying the resulting biomass growth with appropriate techniques, such as quantification of extracted chlorophyll-a or a non-destructive proxy method, such as colour spectrophotometry [29] and pulse amplitude modulated (PAM) chlorophyll fluorometry [30]. Thus, the aim of this study was to investigate the anti-biofouling efficiency (decrease in bioreceptivity) generated on a granite rock surface coated with Si-based consolidants (ethyl silicate or nano-sized silica) to which different concentrations of TiO<sub>2</sub> were added (0, 0.5, 1 and 3%, by wt.), relative to two phototrophic microorganisms: an alga (*Bracteacoccus minor*) and a cyanobacterium (*Nostoc* sp. PCC 9104). In addition, the relationships between the materials added (with concomitant surface changes) and the occurrence of phototrophic microorganisms were established by measuring biomass growth and algal or cyanobacterial dominance.

## 2. Materials and methods

### 2.1. Preparation and inoculation of coated granite samples

Twenty-seven blocks of the commercial granite ‘Rodas’ [for more data on its petrophysical properties, see [31] and [19]], of dimensions 4 cm × 4 cm × 2 cm and with a disc-cut finish, were used in the tests. Blocks were subjected to 500 °C during 12 h and subsequently, they were cooled by tap water jet and placed at laboratory conditions (15 ± 5 °C and RH 60 ± 10%) during two days. This cycle was repeated three times. This procedure affected the physical integrity of the rock [31], and thereby, the open porosity of the blocks was 6.5% [31], which is high in comparison with the open porosity values of 0.1–2% usually observed in sound granitic rocks [32,33].

The upper surface (16-cm<sup>2</sup>) of triplicate samples of each granite block (two groups of 12 samples) was coated with one of the two consolidant products, Estel 1000® or Nano Estel® [31,19], to which different amounts of TiO<sub>2</sub> (Aeroxide P-25, from Evonik Resource Efficiency GmbH, Barcelona, Spain) had been added (0, 0.5, 1 and 3 wt%). Estel 1000® is composed of tetraethyl orthosilicate diluted in white spirit D40 (70 vol%), and Nano Estel® is an aqueous colloidal solution of nanosized silica particles (10–30 nm). The granite samples were coated following the procedure described by Pozo-Antonio et al. [31]. The remaining three granite samples were not treated and were used as controls, for comparative purposes.

After 30 days, the samples were inoculated with a prepared mixture (1:1, w/w) of individual cultures (at exponential growth stage) of the alga *Bracteacoccus minor* (Chlorophyta, Chlorococcales) and of the cyanobacterium *Nostoc* sp. PCC 9104, grown in BG-11 liquid medium [34] (see morphology of species in Fig. S1).

Aliquots (1 mL) of the mixed cell suspension were spread evenly on the upper surface of each granite sample block. The cell concentration

was quantified in an Utermöhl sedimentation chamber [35]. The total cell concentration was  $8.1 \cdot 10^6 \pm 863$  cells mL<sup>-1</sup>; the concentration of *B. minor* was  $3.6 \cdot 10^6 \pm 795$  cells mL<sup>-1</sup>, and the concentration of *Nostoc* sp. PCC 9104 was  $4.5 \cdot 10^6 \pm 921$  cells mL<sup>-1</sup>. The ratio between green alga and cyanobacterium was therefore almost 1:1 in terms of biomass.

### 2.2. Set-up of the bioreceptivity experiment

The inoculated granite samples were maintained for 75 days under stationary conditions in an incubator (INCUDIGIT, J.P SELECTA, Barcelona, Spain), in which a daylight fluorescent lamp (OSRAM L18/865), with a 12 h:12 h light/dark photoperiod regime, provided the following phototrophic growth conditions: 20.3 ± 2.5 °C temperature, 90.2 ± 3.9% relative humidity, and 9.55 ± 0.33 μmol photon m<sup>-2</sup> s<sup>-1</sup> irradiance. These are average values of data recorded every 60 min throughout the entire experimental period using a data logger (HOBO, Onset, USA). Irradiance data measured in the unit Lux were converted according to the formula proposed by Ginzburg [36].

### 2.3. Monitoring phototrophic growth by non-destructive techniques

The upper surface (16 cm<sup>2</sup>) of each granite sample was monitored by digital images and by non-destructive colour and PAM fluorescence measurements, carried out before and after inoculation and every fifteen days over a period of seventy-five days (i.e. on days 15, 30, 45, 60 and 75).

#### 2.3.1. Digital photographs

Digital photographs of all samples were taken with a Nikon D3400 digital camera equipped with Nikon Nikkor Zoom Lens, DX 18-105 mm. The room where the images were taken was totally dark, and a black cloth was placed on the floor under the table used as the sample stand, to minimize background lighting. In addition, the amount of light reaching the target was maintained sufficiently uniform by using the camera-light configuration and methodology described by Sanmartín et al. [37].

#### 2.3.2. Colour spectrophotometry

Colour measurements were made with a portable spectrophotometer (Konica Minolta CM-700d) equipped with CMS100w (SpectraMagicTM NX) software. The working conditions were as follows: medium area view (MAV) 8 mm, illuminant D65, observer 10° and specular component excluded (SCE) mode. This mode provides the best approximation of the colour as visualized by the naked eye and is most sensitive to differences in colour owing to differences in surface roughness [28]. A total of 10 readings were taken at different randomly selected zones [38] on each wet surface block [39], and the results were expressed as mean values. The readings were analyzed using the CIELAB colour system [40], which represents each colour by means of three scalar parameters or Cartesian coordinates: L\*, lightness, which varies from 0 (absolute black) to 100 (absolute white); a\*, associated with changes in redness-greenness (positive a\* is red and negative a\* is green); and b\*, associated with changes in yellowness-blueness (positive b\* is yellow and negative b\* is blue).

#### 2.3.3. Pulse amplitude modulated (PAM) fluorometry

The fluorescence signal of dark-adapted cells (F<sub>0</sub>, the minimal ‘in vivo’ fluorescence signal) at 665 nm (related to the chlorophyll-a content) and the F<sub>v</sub>/F<sub>m</sub> ratio at 665 nm, which describes the quantum photochemical efficiency of PSII and is used to check the vitality of the photosynthetic organisms present [see e.g. [41,42]], were recorded using a multi-wavelength Phyto-PAM fluorometer (Heinz Walz GmbH, Effeltrich, Germany) equipped with a fibre optics emitter-detector unit (PHYTO-EDF). Surface samples were maintained in darkness for at least 20 min and were hydrated prior to the measurements. Sixteen readings were made at randomly selected points on each sample [28] and acquired at gain (G) 13 and PAR: 16.



## 2.4. Analysis at the end of experiment

### 2.4.1. Stereoscopic and scanning electron microscopy

The upper surface of samples was analyzed in detail, before inoculation and at the end of the experiment, using an Olympus SZX7 zoom stereomicroscope. In addition, at the end of the experiment and after the removal of biological colonization to extract the photosynthetic pigments (Section 2.4.2), the coated surfaces were examined by Scanning Electron Microscopy (SEM), using a Philips XL30 coupled with an energy dispersive X-ray spectrometry (EDS) in secondary electron (SE) and backscattered electron (BSE) modes.

### 2.4.2. Extraction and determination of photosynthetic pigments

Chlorophyll-a, chlorophyll-b, total carotenoids and scytonemin were extracted using the protocol reported by Fernández-Silva et al. [43] for extraction of photosynthetic pigments from granite rock, with slight modifications. Thus, each sample was placed upside down in a Petri dish containing 6.88 mL of DMSO (i.e. with the inoculated surface touching the bottom of plate). The sample was then sonicated by inserting the narrow tip of an ultrasonic generator (Sonics Vibra-cell) into the extractant for  $5 \times 20$  s (40% amplitude), with 5 s breaks to prevent overheating, followed by incubation at 63 degrees for 40 min. The extracts were then collected, filtered and measured in a UV Visible Spectrophotometer (Varian Cary 100). The equations proposed by Wellburn [44] were used to determine the concentrations of chlorophyll-a and chlorophyll-b, while the amount of scytonemin was quantified using the equation of García-Pichel and Castenholz [45]. The ratio of absorbances of the extracts at 435 and 415 nm ( $A_{435}/A_{415}$ ) was interpreted as the phaeophytinization quotient, which reflects the degradation of chlorophyll to phaeopigments [46].

## 2.5. Statistical analysis

The data were subjected to analysis of variance (ANOVA), a post hoc HSD Tukey test and Student's *t*-test (for paired comparison), all of which were implemented in the SPSS statistical programme (version 22.0). A significance level of 5% was applied ( $p$ -value  $\leq 0.05$ ).

## 3. Results

The visual changes in the biological colonization on the samples, documented by means of digital photographs (Fig. 1), clearly revealed growth of the phototrophic microorganisms inoculated on the untreated samples, which acquired an increasingly greenish coloration throughout the experiment. By contrast, the amount of  $\text{TiO}_2$  added to the consolidant was not correlated with the level of colonization on the surface of the treated samples. Thus, for example, greening was more evident in some samples coated with Nano Estel® containing 1% of  $\text{TiO}_2$  and in other samples coated with Estel 1000® containing 3% of  $\text{TiO}_2$  than in samples coated with consolidants containing 0.5% of  $\text{TiO}_2$  or even those to which  $\text{TiO}_2$  was not added. Macroscopic photographs also show the whitening that the  $\text{TiO}_2$  caused on the surfaces, especially in the consolidant containing 3%  $\text{TiO}_2$ .

Detailed stereomicroscope images (Fig. 2) enabled detection of where the growth of the microorganisms was taking place, and also which of the two consolidants (based on ethyl silicate or nanosized silica) most favoured growth of the microorganisms. Greening was clearly visible inside the cracks created by the consolidant, as noted in images of samples coated with Estel 1000® containing 3%  $\text{TiO}_2$  and Nano Estel® containing 1%  $\text{TiO}_2$ , and visible greening was also noted in the macroscopic images (Fig. 1). In addition, the phototrophic growth on samples coated with Nano Estel® was greater than on samples coated with Estel 1000®, regardless of the amount of  $\text{TiO}_2$  added.

Subsequent SEM-EDS studies revealed further details of the characteristics of the cracks. SEM images revealed homogeneous dispersion of  $\text{TiO}_2$  in both consolidants and also differences between treatments in the

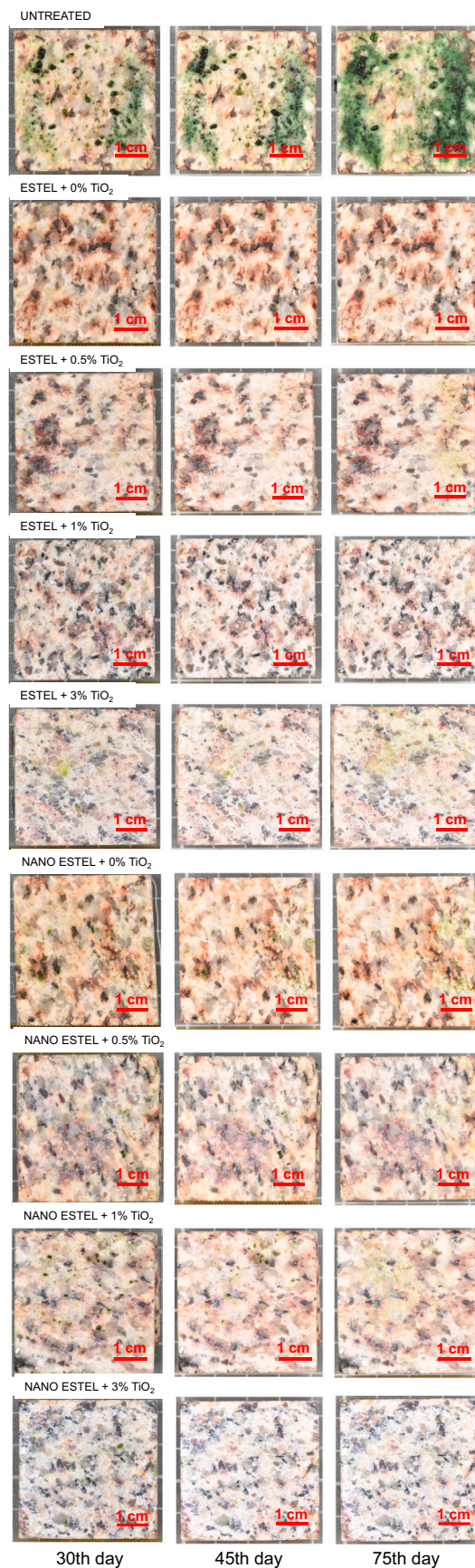


Fig. 1. Macroscopic appearance of the surface of the samples throughout the experimental period.



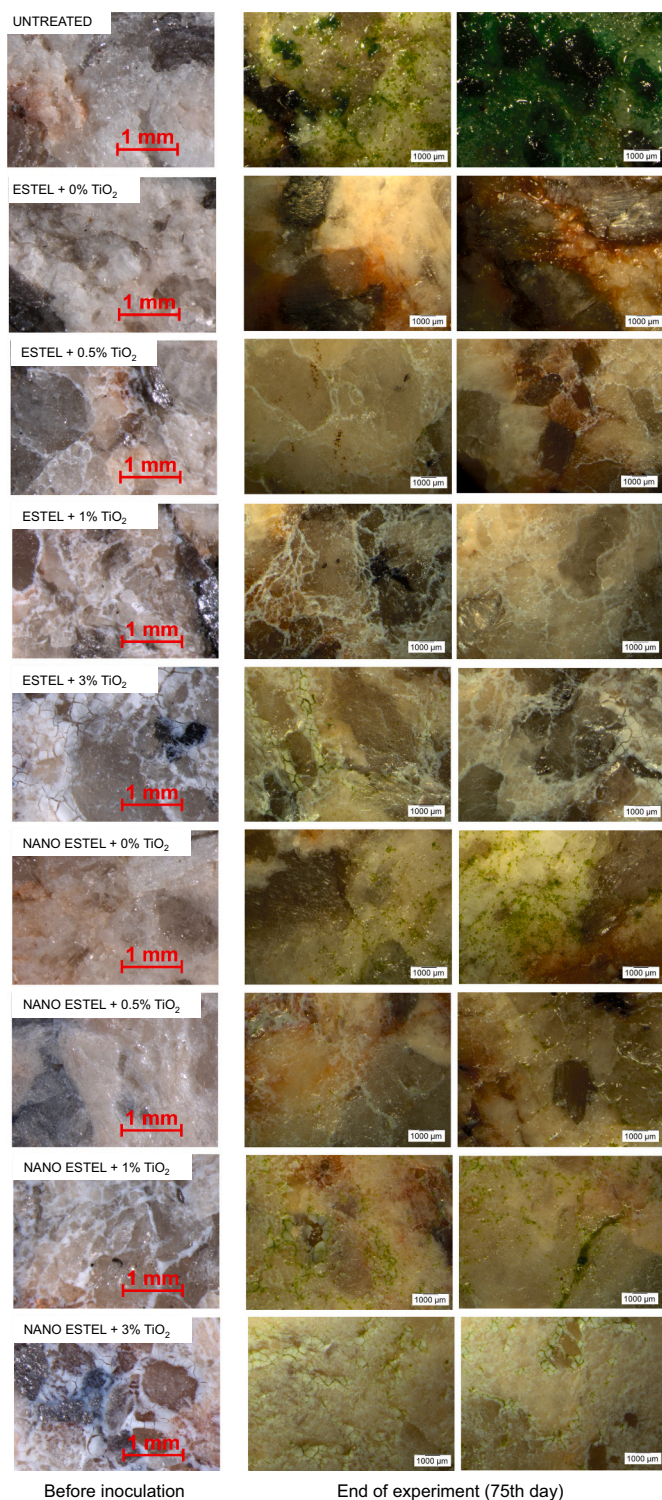


Fig. 2. Stereoscopic photomicrographs of different areas of the surface of the samples.

cracking pattern, with wider and more abundant cracks in the ethyl silicate matrix and fewer, narrower cracks in the nano-sized Si matrix (Fig. 3). EDS analysis also demonstrated that the cracks reached the surface of the granite rock, becoming areas of lower biocidal activity, as no consolidant containing  $\text{TiO}_2$  was detected (Fig. 3).

The changes in CIELAB coordinates  $L^*$ ,  $a^*$  and  $b^*$  are shown in Fig. 4. Regarding  $L^*$ , the values for all samples (including the untreated samples), ranging from 69 to 78 CIELAB units, indicated light colouration of

the surfaces before inoculation. The differences between groups of samples were maintained after inoculation, and a similar decrease in  $L^*$  of around 16 CIELAB units was observed in all cases. However, it was not identified a pattern of a continuous increase or decrease over time. At the end of experiment, the values for samples coated with consolidants containing the highest amount of  $\text{TiO}_2$  (3% in both) corresponded to the lightest or whitest surfaces, followed by those of both consolidants containing 1%  $\text{TiO}_2$ . The samples coated with either consolidant containing the lowest amounts of  $\text{TiO}_2$  (0 and 0.5%) were darker. Within these 3 groups (formed in accordance with the amount of  $\text{TiO}_2$ ), there were no significant differences between Estel 1000® and Nano Estel®. The changes in lightness over time were significant, in the samples treated with consolidant containing the highest amount of  $\text{TiO}_2$  (3% and 1%) and previously in the samples with Nano Estel®.

The value of the chromatic parameter  $a^*$  (associated with red-green hues) decreased as the phototrophic colonization developed, as observed in the untreated samples, but the decrease was only significant at the end of experiment (Fig. 4). The inoculation generated significant differences between groups of samples in relation to the surface greening; however, differences in the  $a^*$  value on the samples surface were not significant either before inoculation or at the end of experiment.

The chromatic parameter  $b^*$  (associated with yellow-blue hues) increased (significantly from 60th day of experiment) during development of phototrophic colonization, as observed in the untreated samples (Fig. 4). The values of  $b^*$  for the groups of samples before and after the inoculation were significantly different. At the end of experiment, the samples were grouped similarly according to the concentration of  $\text{TiO}_2$ , but in the opposite way to parameter  $L^*$ . Furthermore, in the samples treated with Estel 1000® there was a significant decrease in  $b^*$  - associated with a decrease in colonization - from the measurement following inoculation (day 15), which was not observed in the samples treated with Nano Estel®.

The fluorescence  $F_0$  values at 665 nm are shown in Fig. 5. Untreated samples yielded high  $F_0$  values, which tended to increase towards the end of experiment (on day 60 and 75). The treated samples yielded lower values than the untreated samples and differed significantly after inoculation; the samples treated with Estel 1000® yielded lower  $F_0$  values than the samples treated with Nano Estel®, regardless of the  $\text{TiO}_2$  content. The  $F_0$  decreased in all treated samples throughout the study period, with a slight recovery in the samples treated with Nano Estel® from day 60. At the end of experiment, for the same amount of  $\text{TiO}_2$ , the  $F_0$  values were higher in samples treated with the Nano Estel® than in those treated with Estel 1000®.

The photosynthetic yield, expressed in terms of  $F_v/F_m$  (Fig. 5), showed that although there were no notable differences between the samples after inoculation, not even relative to the untreated samples, this changed over time. Thus, at the end of experiment, for equal concentrations of  $\text{TiO}_2$ , the samples treated with Nano Estel®, the photosynthetic yield was similar to that obtained in the untreated samples and higher than in the samples treated with Estel 1000®.

Pigment extraction at the end of experiment (Fig. 6) showed that the untreated samples produced significantly more chlorophyll-a, which can be considered an estimator of biomass [see e.g. [43]], than the treated samples. Notable amounts of chlorophyll-b and a very low amount of scytonemin were detected in all samples. The amount of chlorophyll-b on the samples differed significantly, with higher values for the untreated samples, Estel 1000® with 3%  $\text{TiO}_2$  and Nano Estel® with 0% and 0.5%  $\text{TiO}_2$ . The amount of scytonemin was higher in Nano Estel® than in Estel 1000®, although the differences were not significant. Production of chlorophyll-a, chlorophyll-b, and scytonemin in the samples treated with consolidants containing 1%  $\text{TiO}_2$  differed significantly, and in the case of scytonemin also for the consolidants with 0%  $\text{TiO}_2$ . In addition, Nano Estel® caused less degradation of chlorophyll-a than Estel 1000®, as a decrease in the phaeophytinization quotient indicates increased degradation of chlorophyll to phaeopigments [46,47].



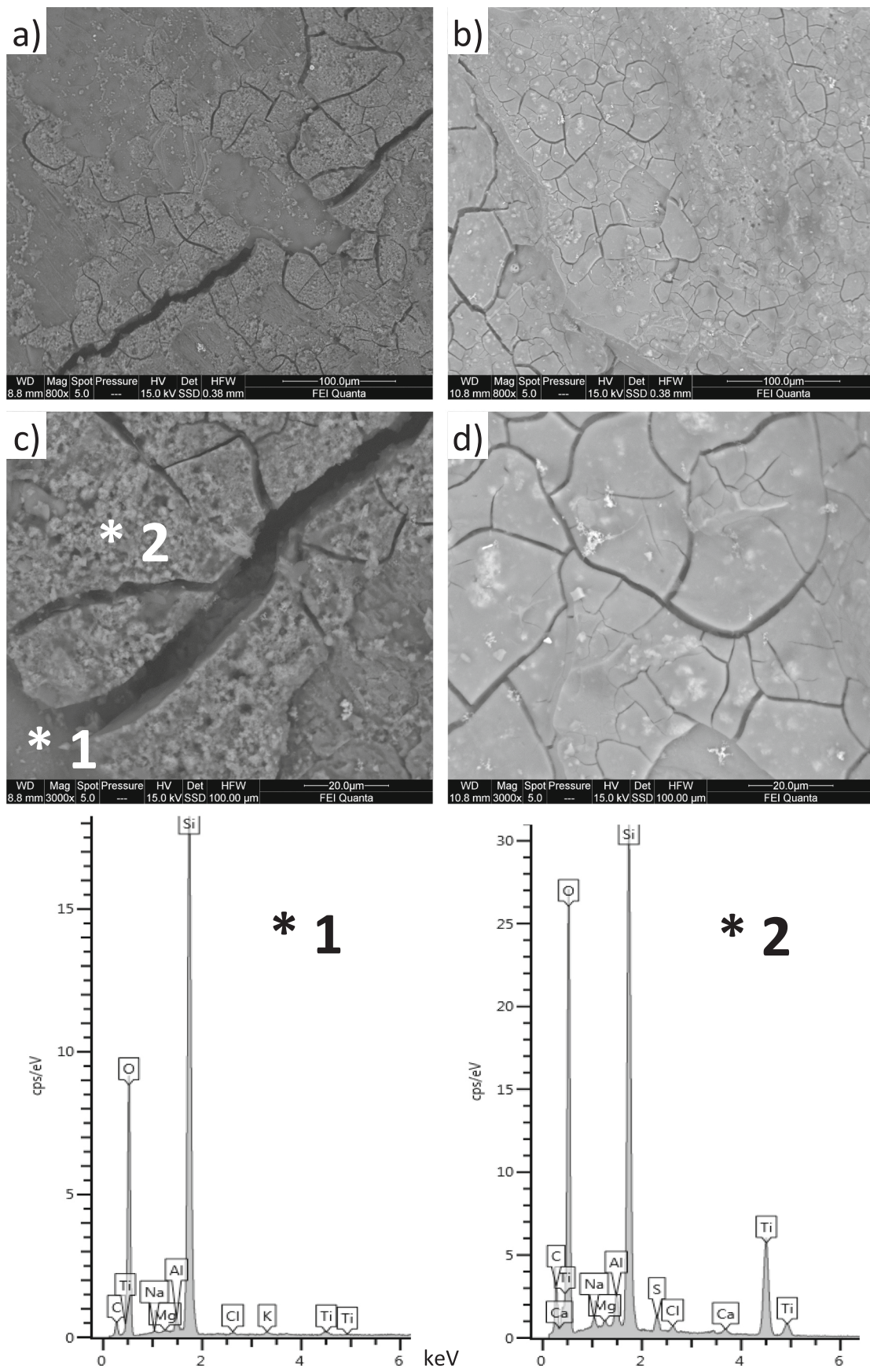
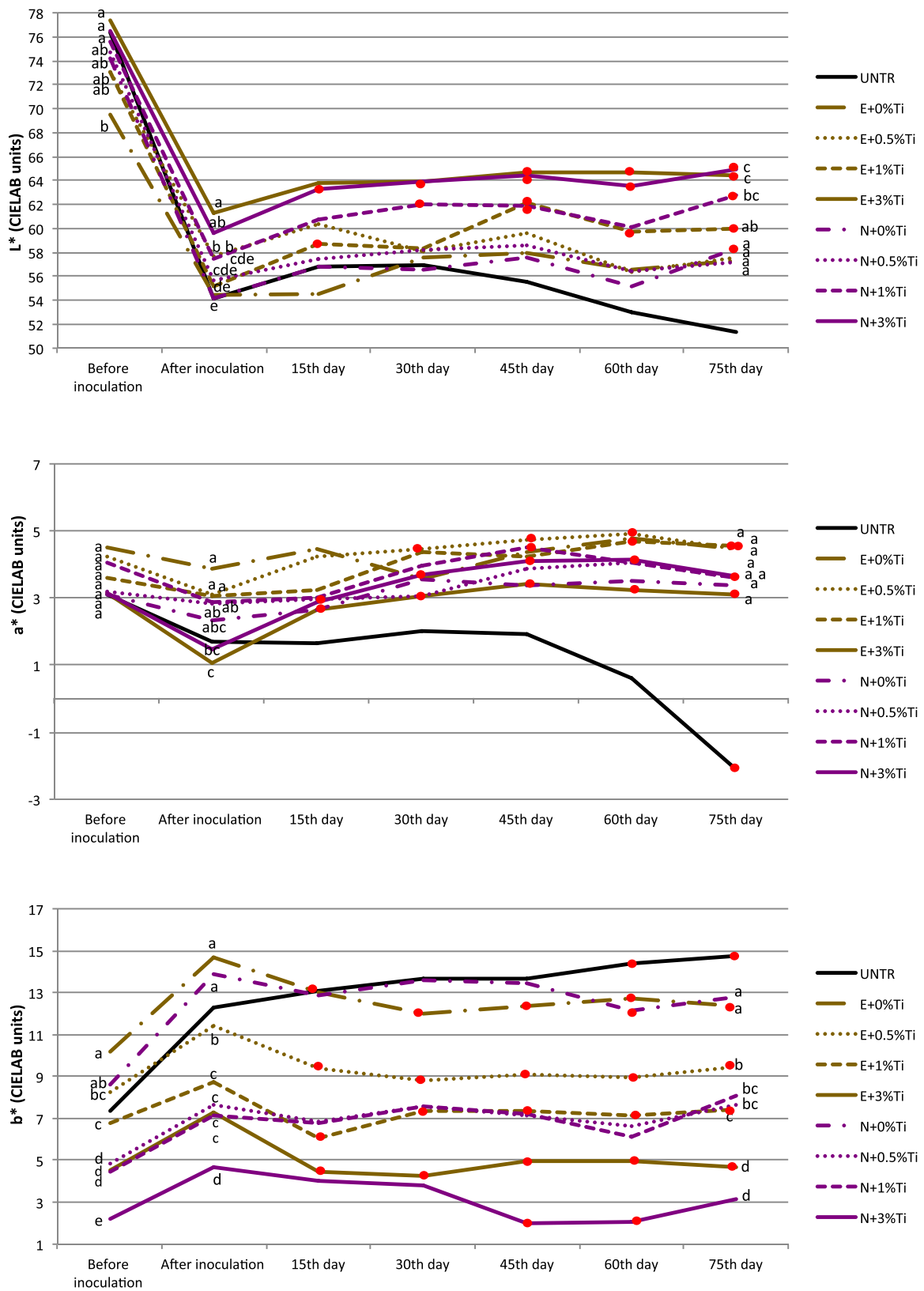
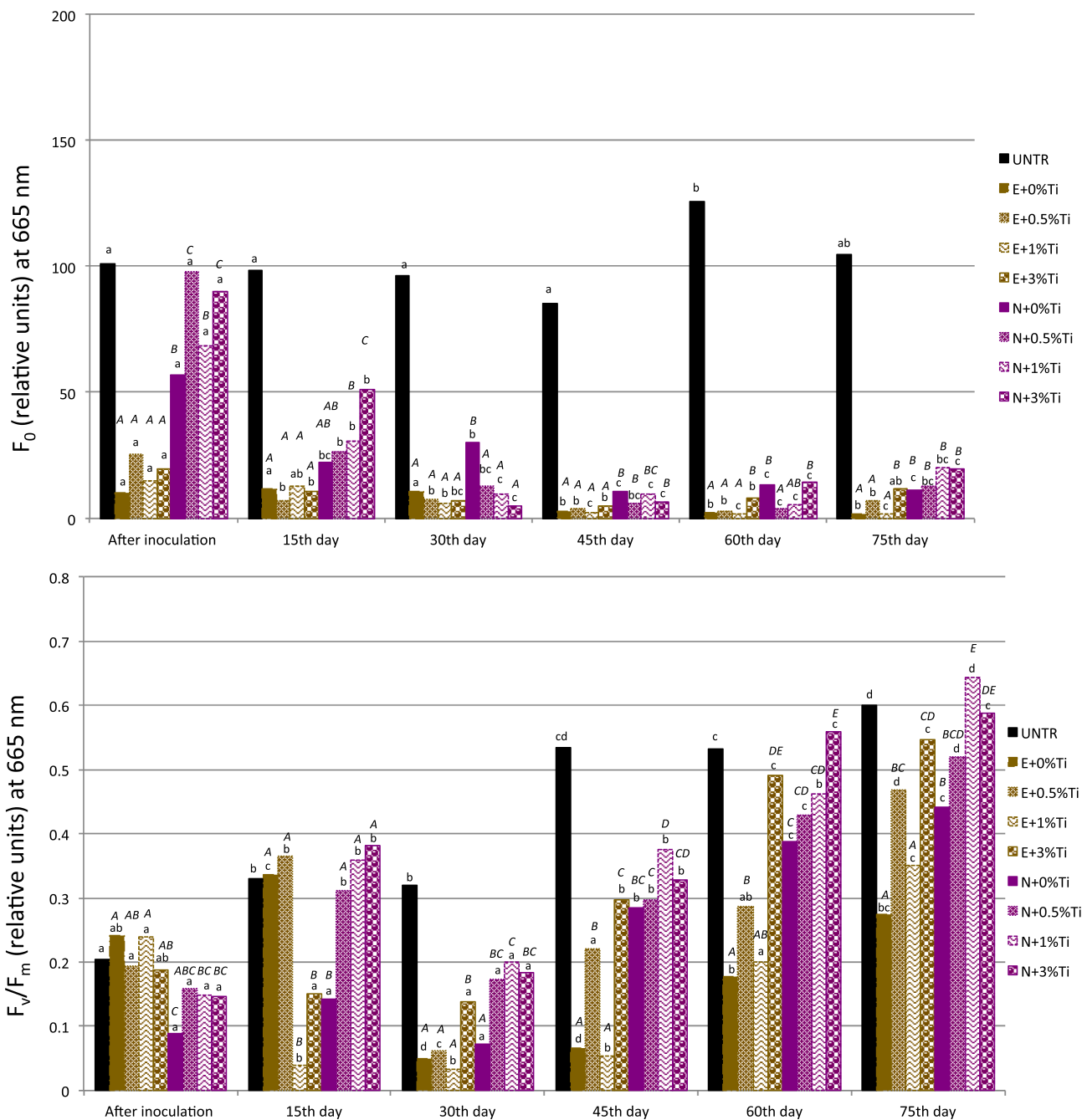


Fig. 3. SEM micrographs of the surfaces coated with Estel 1000® (a, c) and Nano Estel® (b, d) containing 0.5% TiO<sub>2</sub> (wt%) after removal of the incipient biological colonization for pigment extraction. \*1 (fracture/crack) and \*2 (coating) indicate the points where EDS spectra were obtained.



**Fig. 4.** CIELAB colour data. Values of L\* (lightness), a\* (red-green changes) and b\* (yellow-blue changes) on the upper surface of the samples throughout the experimental period. Data points represent the average of three replicates. Red dots indicate significant differences in each group of samples relative to the beginning of the experiment (after inoculation) at each measurement time point. Different letters at three time points (before and after inoculation and at the end of experiment – day 75 day –) indicate significant differences between the eight groups of treated samples. (For interpretation of the references to colour in this figure legend, the reader is referred to the web version of this article.)





**Fig. 5.**  $F_0$  (minimal fluorescence signal of dark-adapted cells) and  $F_v/F_m$  (quantum photochemical efficiency of PSII) at 665 nm for the upper surface of the samples throughout the experimental period. The histograms represent mean values of three replicates. Different lowercase letters indicate significant differences in each group of samples at different times. Different uppercase letters indicate significant differences between the eight groups of treated samples for each measurement time.

#### 4. Discussion

This case study of extrinsic bioreceptivity, as defined by Guillitte [1], and quaternary bioreceptivity, as defined by Sanmartín et al. [2], was addressed by examining how the application of different consolidants (based on ethyl silicate, Estel 1000®, or nano-sized silica, Nano Estel®, to which different amounts of  $TiO_2$  were added) to the material under study (granite rock) affected the establishment, anchorage and development of biological colonization.

Since the 1970s, polymers and synthetic protective materials have been used in an attempt to enhance the long-term preservation of buildings, especially monuments, [48]. In this context, there is currently

a trend for using  $TiO_2$ -based consolidants to treat cultural heritage monuments and civil buildings because of their self-cleaning and anti-biofouling performance under UV irradiation [49,20,50,19]. However, although case studies reported favourable results [e.g. [51]], the first drawbacks of the  $TiO_2$ -based coatings are beginning to emerge. For example, according to Quagliarini et al. [20] high roughness and porosity on the surface of stones such as limestones, sandstones and tuffs, widely used in cultural heritage, seem to contribute to the formation of cracks in the coatings. In the present study, the  $TiO_2$ -containing consolidants applied to granite (with much lower porosity than limestones, sandstones and tuffs) developed cracks which were less abundant and narrower in Nano Estel® than in Estel 1000®, regardless

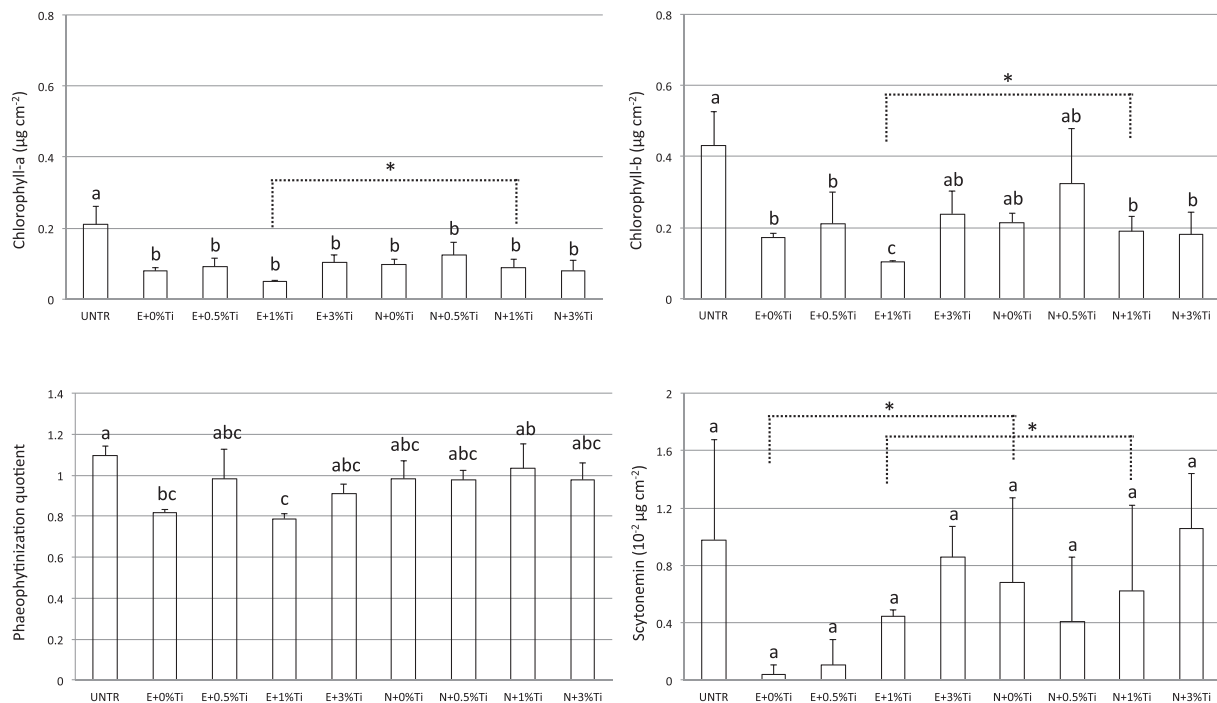


**Fig. 6.** Chlorophyll-a, chlorophyll-b, phaeophytization quotient and scytonemin production at the end of the experiment. The histograms represent mean values of three replicates (bars represent the SD). Different letters indicate significant differences between the nine groups of samples (including untreated samples). Asterisks indicate significant differences in each pair of samples treated with different consolidants (Estel 1000® or Nano Estel®) but the same percentage of TiO<sub>2</sub>. Untr: untreated, E: Estel 1000® (based on ethyl silicate), N: Nano Estel® (based on nanosized silica), Ti: TiO<sub>2</sub>.

of the amount of TiO<sub>2</sub> added.

It has been known since the first studies were carried out [21] that bioreceptivity to pioneer colonizing organisms (i.e. cyanobacteria, green algae, diatoms and mosses) is primarily determined by surface roughness, porosity and the chemical nature of the material being colonized [25] and references therein]. However, the relative impact of the three factors on bioreceptivity is not yet clear [2]. Barberousse et al. [52] made some progress in this regard, showing that the bioreceptivity of rough materials is four times higher than that of smooth materials. D’Orazio et al. [22] constructed a polynomial curve correlating the water retention (and in turn nutrient retention) on a material (due to its roughness and total porosity) with the biological colonization level (expressed as chlorophyll fluorescence intensity of biofilm cells). According to these authors, as more water is retained inside the fissures and voids on the surface, the growth of algal biofilms on the surface will increase, up to a certain point where the growth curve stabilizes. Similarly, Quagliariini et al. [20] demonstrated the limited efficiency of TiO<sub>2</sub> to protect against algal proliferation, because cracks in the coating enable anchorage of algal cells (accelerating the adhesion of microorganisms and formation of biofilm) and contribute to retention of water and nutrients in the substrate.

Thus, in the present study we expected that more abundant and wider cracking would retain more water, which would favour the development of colonization, in turn, leading to higher bioreceptivity. Ruffolo et al. [53] applying an aqueous dispersion of nanosilica undoped and doped with TiO<sub>2</sub> on a stonewall partially plastered after a biocide treatment found that the dispersion added regardless of the TiO<sub>2</sub> content (undoped and doped TiO<sub>2</sub>) reduced the potential new recolonization. A higher recolonization rate occurred on the portions with greater humidity. Therefore, water reduced the efficacy of titanium dioxide. Ruffolo et al. [54] working on the application of metal oxide nanoparticles dispersed in siloxane wax on stone surfaces underwater found that the wax itself induces a decrease of stone roughness and subsequently reduces the adhesion dynamics of the fouling on the surface. Therefore, the presence of fractures would facilitate such adhesion. However, the

colour parameter b\* and F<sub>0</sub> at 665 nm showed that retention of microorganisms was greater after inoculation of the samples with Nano Estel®. The colour parameter L\* did not show a clear trend because it is related to the heterogeneous biological colonization showing different extents on the surface. The narrower fractures generated in this coating seem to favour anchorage and retention of the phototrophs, which, being more abundant, also develop further, as shown by the stereoscopic photomicrographs, and in more favourable physiological conditions, as shown by the Fv/fm ratio at 665 nm and the phaeophytization coefficient. This could be explained because narrower fractures favour water retention closer to the surface since there is less loss to deeper areas and in addition produces a greater retention of organisms at the surface proximity. This causes the organisms, which are more retained on the surface, to be exposed to light to a greater extent than those in the crack (Fig. 7). Light is a key factor for their development as it regulates growth and physiological processes in photosynthetic organisms. Indeed, light is a type of electromagnetic radiation that, via photochemical interactions, provides the main source of energy for the metabolism of photoautotrophic organisms (i.e. photosynthesis) and that is directly involved in fixing C, and in N and S metabolism [55]. In turn, the increased water availability leads to a better metabolic state of the organisms. Both factors together could explain the higher development of organisms in the narrow fracture zones developed by Nano Estel®. The initial difference would modify the bioreceptivity of the coated granite, so that the results of the biocidal action of TiO<sub>2</sub> would be mediated by the relative abundance of organisms. In addition, the larger layer of organisms on the surface could act as a screen for the passage of light, interacting with TiO<sub>2</sub> and reducing its photocatalytic efficiency, provoking even more differences between treatments.

Algae depend on water availability to a much greater extent than cyanobacteria, which display varying abilities to resist desiccation [52,56]. This may explain why algae (associated with the high values of chlorophyll-b) were more abundant than cyanobacteria (associated with low values of scytonemin) in the biological colonization developed on the surface of the samples. In addition, the morphology of the algal cells



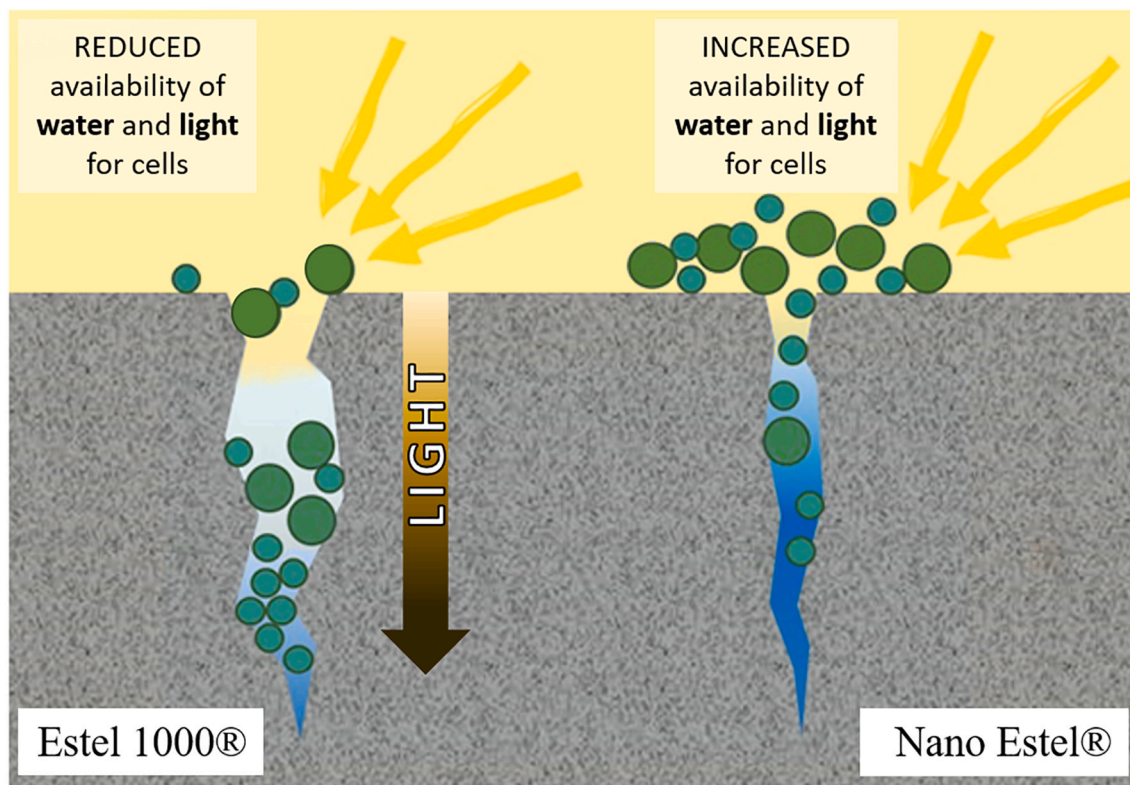


Fig. 7. Graphical representation of the behavior of microorganisms according to the surfaces.

and their size facilitated attachment within the cracks, while cyanobacterial cells may have been lost despite spread more easily on the sample surface. Comparison of the levels of scytonemin in both consolidants with the same amount of  $\text{TiO}_2$  revealed that Nano Estel® contained a higher proportion of this pigment (although the difference was not significant). This may be due to the fact that the wider cracks caused by Estel 1000® favoured loss of the smaller cyanobacteria, while the narrower cracks produced by Nano Estel® would favour anchorage.

## 5. Conclusions

The results appear to confirm that added materials such as coatings are important in the process of microbial colonization on surfaces, because of their own bioreceptivity. As previously in rough, highly porous stony materials (such as limestone, sandstone and tuff, with a porosity ranging from 15 to 40%), in the present paper we have shown for the first time in a much less porous material, such as granite with a porosity of 6.5%, how the application of coating treatments containing  $\text{TiO}_2$  causes the formation of micro cracks that strongly promote biofouling, thus overwhelming the biocidal power of  $\text{TiO}_2$ . Furthermore, although the cracks in ethyl silicate were more abundant and wider, nanosized silica provided better anchorage points, making the material treated with the consolidant containing nanosized Si more bioreceptive to microbial colonization. This could be explained because narrower fractures favour water retention closer to the surface since there is less loss to deeper areas and in addition produces a greater retention of organisms at the surface proximity. This causes the organisms, which are more retained on the surface, to be exposed to light to a greater extent than those in the crack.

Supplementary data to this article can be found online at <https://doi.org/10.1016/j.msec.2021.112058>.

## Declaration of competing interest

The authors declare that they have no conflicts of interest.

## Acknowledgements

The authors thank Rafael Carballeira (Universidade da Coruña) for photographs and analysis of the inoculum. P. Sanmartín and E. Fuentes are grateful to the Xunta de Galicia for the financial support awarded (grant ED431C 2018/32). E. Fuentes is also financially supported by a PhD Fellowship-Contract MICINN-FPI (BES-2017-079927). J.S. Pozo-Antonio thanks the Spanish Ministry of Economy and Competitiveness (MINECO) for a Juan de la Cierva-Incorporación (IJCI-2017-3277) post-doctoral contract.

## CRediT authorship contribution statement

**P. Sanmartín:** Conceptualisation, Formal analysis, Methodology, Resources, Validation, Visualisation, Writing - original draft, Writing - review & editing, Supervision. **D. Noya-Pintos:** Formal analysis, Investigation, Validation, Visualisation, Writing - original draft. **E. Fuentes:** Validation, Visualisation, Writing - original draft. **J.S. Pozo-Antonio:** Conceptualisation, Formal analysis, Methodology, Resources, Validation, Visualisation, Writing - original draft, Writing - review & editing, Supervision.

## References

- [1] O. Guillitte, *Bioreceptivity: a new concept for building ecology studies*, *Science of the Total Environment* 167 (1995) 215–220.
- [2] P. Sanmartín, A.Z. Miller, B. Prieto, H. Viles, *Revisiting and reanalysing the concept of bioreceptivity 25 years on*, *Science of the Total Environment* 770 (2021) 145,314.
- [3] R.J. Koestler, E.D. Santoro, *Assessment of the Susceptibility to Biodeterioration of Selected Polymers and Resins*, The Getty Conservation Institute, Bloomfield, 1988.

- [4] G. Caneva, M.P. Nugari, Evaluation of Escobilla's mucilagino treatments in the archaeological site of Joya de Ceren (El Salvador), in: B.O. Ortega-Morales, C. C. Gaylarde, J.A. Narvaez-Zapata, P.M. Gaylarde (Eds.), LABS5. Biodegradation and Biodeterioration in Latin America, Universidad de Campeche, Mexico, 2005, pp. 59–64.
- [5] F. Cappitelli, E. Zanardini, C. Sorlini, The biodeterioration of synthetic resins used in conservation, *Macromolecular Bioscience* 4 (2004) 399–406.
- [6] F. Cappitelli, J.D. Nosanchuk, A. Casadevall, L. Toniolo, L. Brusetti, S. Florio, P. Principi, S. Borin, C. Sorlini, Synthetic consolidants attacked by melanin-producing fungi: case study of the biodeterioration of Milan (Italy) Cathedral marble treated with acrylics, *Applied and Environmental Microbiology* 73 (1) (2007) 271–277.
- [7] F. Cappitelli, P. Principi, R. Pedrazzani, L. Toniolo, C. Sorlini, Bacterial and fungal deterioration of the Milan Cathedral marble treated with protective synthetic resins, *Science of the Total Environment* 385 (1–3) (2007) 172–181.
- [8] C. Urzi, F. De Leo, L. Krakova, D. Pangallo, L. Bruno, Effects of biocide treatments on the biofilm community in Domitilla's catacombs in Rome, *Science of the Total Environment* 572 (2016) 252–262.
- [9] P. Sanmartín, R. Carballeira, Changes in heterotrophic microbial communities induced by biocidal treatments in the Monastery of San Martiño Pinarío (Santiago de Compostela, NW Spain), *International Biodeterioration and Biodegradation* 156 (2021) 105130.
- [10] S. Scheerer, O. Ortega-Morales, C. Gaylarde, Microbial deterioration of stone monuments—an updated overview, *Advances in Applied Microbiology* 66 (2009) 97–139.
- [11] V. Jurado, A. Miller, S. Cuezva, A. Fernandez-Cortes, D. Benavente, M. Rogerio-Candelera, J. Reyes, J. Cañaveras, S. Sanchez-Moral, C. Saiz-Jimenez, Recolonization of mortars by endolithic organisms on the walls of San Roque church in Campeche (Mexico): a case of tertiary bioreceptivity, *Construction and Building Materials* 53 (2014) 348–359.
- [12] E. Diakumaku, A.A. Gorbushina, W.E. Krumbein, L. Panina, S. Soukharjevski, Black fungi in marble and limestones—an aesthetical, chemical and physical problem for the conservation of monuments, *Science of the Total Environment* 167 (1995) 295–304.
- [13] U. Wollenzien, G.S. de Hoog, W.E. Krumbein, C. Urzi, On the isolation of microcolonial fungi occurring on and in marble and other calcareous rocks, *Science of the Total Environment* 167 (1995) 287–294.
- [14] D. Pinna, O. Salvadori, Biological growth on Italian monuments restored with organic or carbonatic compounds, in: O. Ciferri, G. Mastromei, P. Tiano (Eds.), *Of Microbes and Art: The Role of Microbial Communities in the Degradation and Protection of Cultural Heritage*, Plenum Publishers, New York, NY, 1999, pp. 149–154.
- [15] J. Brush, P. Kotlik, Cracking of organosilicone stone consolidants in gel form, *Studies in Conservation* 41 (1996) 55–59.
- [16] M.J. Mosquera, J. Pozo, L. Esquivias, Stress during drying of two stone consolidants applied in monumental conservation, *Journal of Sol-Gel Science and Technology* 26 (2003) 1227–1231.
- [17] Mosquera, M.J., de los Santos, D.M., Rivas, T., Sanmartín, P., Silva, B., 2009. New nanomaterials for protecting and consolidating stone. *Journal of Nano Research* 8, 1–12.
- [18] A. Sierra-Fernández, L.S. Gomez-Villalba, M.E. Rabanal, R. Fort, New nanomaterials for applications in conservation and restoration of stony materials: a review, *Materiales de Construcción* 67 (325) (2017) 107.
- [19] J.S. Pozo-Antonio, D. Noya-Pintos, P. Sanmartín, Moving towards smart cities: evaluation of the self-cleaning properties of Si-based consolidants containing nanocrystalline TiO<sub>2</sub> activated by either UV-A or UV-B radiation, *Polymers* 12 (11) (2020) 2577.
- [20] E. Quagliarini, L. Graziani, D. Diso, A. Licciulli, M. D'Orazio, Is nano-TiO<sub>2</sub> alone an effective strategy for the maintenance of stones in cultural heritage? *Journal of Cultural Heritage* 30 (2018) 81–91.
- [21] O. Guillitte, R. Dreesen, Laboratory chamber studies and petrographical analysis as bioreceptivity assessment tools of building materials, *Science of the Total Environment* 167 (1995) 365–374.
- [22] M. D'Orazio, G. Cursio, L. Graziani, L. Aquilanti, A. Osimani, F. Clementi, C. Yéprémian, V. Lariccia, S. Amoroso, Effects of water absorption and surface roughness on the bioreceptivity of ETICS compared to clay bricks, *Building and Environment* 77 (2014) 20–28.
- [23] H. Barberousse, R.J. Lombargo, G. Tell, A. Couté, Factors involved in the colonisation of building facades by algae and cyanobacteria in France, *Biofouling* 22 (2) (2006) 69–77.
- [24] B. Prieto, B. Silva, Estimation of the potential bioreceptivity of granitic rocks from their intrinsic properties, *International Biodeterioration and Biodegradation* 56 (2005) 206–215.
- [25] A.Z. Miller, P. Sanmartín, L. Pereira-Pardo, C. Saiz-Jimenez, A. Dionísio, M. F. Macedo, B. Prieto, Bioreceptivity of building stones: a review, *Science of the Total Environment* 426 (2012) 1–12.
- [26] V. Ferrándiz-Mas, T. Bond, Z. Zhang, J. Melchiorri, C.R. Cheeseman, Optimising the bioreceptivity of porous glass tiles based on colonization by the alga *Chlorella vulgaris*, *Science of the Total Environment* 563–564 (2016) 71–80.
- [27] D. Vázquez-Nion, B. Silva, B. Prieto, Bioreceptivity index for granitic rocks used as construction material, *Science of the Total Environment* 633 (2018) 112–121.
- [28] P. Sanmartín, R. Grove, R. Carballeira, H. Viles, Impact of colour on the bioreceptivity of granite to the green alga *Apatococcus lobatus*: laboratory and field testing, *Science of the Total Environment* 745 (2020) 141179.
- [29] D. Vázquez-Nion, P. Sanmartín, B. Silva, B. Prieto, Reliability of color measurements for monitoring pigment content in a biofilm-forming cyanobacterium, *International Biodeterioration and Biodegradation* 84 (2013) 220–226.
- [30] Schreiber, U., 2004. Pulse-amplitude-modulation (PAM) Fluorometry and saturation pulse method: an overview. G.C. Papageorgiou, Govindjee (Eds.), *Chlorophyll Fluoresc. Signal. Photosynth*, Springer Netherlands, Dordrecht, pp. 279–319.
- [31] J.S. Pozo-Antonio, D. Noya, C. Montojo, Aesthetic effects on granite of adding nanoparticle TiO<sub>2</sub> to Si-based consolidants (ethyl silicate or nano-sized silica), *Coatings* 10 (3) (2020) 215.
- [32] A. Rojo, F.J. Alonso, R.M. Esbert, Hydric properties of some Iberian ornamental granites with different superficial finishes: a petrophysical interpretation, *Materiales de Construcción* 53 (269) (2003) 61–74.
- [33] B. Silva, P. Sanmartín, B. Prieto, Characterization of the support rock of the petroglyphs of campo lameiro (Pontevedra), *Cadernos do Laboratorio Xeolóxico de Laxe* 41 (2019) 141–152 (In Spanish). ISSN: 0213-4497.
- [34] Rippka, R., Deruelles, J., Waterbury, J.B., Herdman, M., Stanier, R.Y., 1979. Generic assignments, strain histories and properties of pure cultures of cyanobacteria. *Journal of General Microbiology* 111, 1–61.
- [35] H. Utermöhl, Zur Vervollkommnung der quantitativen Phytoplankton-Methodik, *Mitt. Int. Ver. Ther. Angew. Limnol.* 9 (1958) 1–38.
- [36] M. Ginzburg, *Dunaliella*: a green alga adapted to salt, *Advances in Botanical Research* 14 (1987) 93–183.
- [37] P. Sanmartín, E. Chorro, D. Vázquez-Nion, F.M. Martínez-Verdú, B. Prieto, Conversion of a digital camera into a non-contact colorimeter for use in stone cultural heritage: the application case to Spanish granites, *Measurement* 56 (2014) 194–202.
- [38] B. Prieto, P. Sanmartín, B. Silva, F. Martínez-Verdú, Measuring de the color of granite rocks. A proposed procedure, *Color Research and Application* 35 (5) (2010) 368–375.
- [39] B. Prieto, P. Sanmartín, N. Aira, B. Silva, Color of cyanobacteria: some methodological aspects, *Applied Optics* 49 (11) (2010) 2022–2029.
- [40] CIE S014-4/E:2007. *Colorimetry Part 4: CIE 1976 L\*a\*b\* Colour Space*, Commission Internationale de l'éclairage, CIE Central Bureau, Vienna, 2007.
- [41] S.E. Favero-Longo, R. Benesperi, S. Bertuzzi, E. Bianchi, G. Buffa, P. Giordani, S. Loppi, P. Malaspina, E. Matteucci, L. Paoli, S. Ravera, A. Roccardi, A. Segimiro, A. Vannini, Species- and site-specific efficacy of commercial biocides and application solvents against lichens, *International Biodeterioration and Biodegradation* 123 (2017) 127–137.
- [42] J.S. Pozo-Antonio, P. Sanmartín, Exposure to artificial daylight or UV-irradiation (A, B or C) prior to chemical cleaning: an effective combination for removing phototrophs from granite, *Biofouling* 34 (8) (2018) 851–869.
- [43] I. Fernández-Silva, P. Sanmartín, B. Silva, A. Moldes, B. Prieto, Quantification of phototrophic biomass on rocks: optimization of chlorophyll-a extraction by response surface methodology, *Journal of Industrial Microbiology and Biotechnology* 38 (2011) 179–188.
- [44] A.R. Wellburn, The spectral determination of chlorophylls a and b, as well as total carotenoids, using various solvents with spectrophotometers of different resolutions, *Journal of Plant Physiology* 144 (1994) 307–313.
- [45] F. García-Pichel, R.W. Castenholz, Characterization and biological implications of Scytonemin, a cyanobacterial sheath pigment, *Journal of Phycology* 27 (1991) 395–409.
- [46] R. Ronen, M. Galun, Pigment extraction from lichens with dimethyl sulfoxide (DMSO) and estimation of chlorophyll degradation, *Environmental and Experimental Botany* 24 (1984) 239–245.
- [47] P. Sanmartín, F. Villa, B. Silva, F. Cappitelli, B. Prieto, Color measurements as a reliable method for estimating chlorophyll degradation to phaeopigments, *Biodegradation* 22 (4) (2011) 763–771.
- [48] E. Doehne, C.A. Price, *Stone Conservation—An Overview of Current Research*, 2nd ed., The Getty Conservation Institute, Los Angeles, CA, USA, 2010.
- [49] M.F. La Russa, S.A. Ruffolo, N. Rovella, C.M. Belfiore, A.M. Palermo, M.T. Guzzi, G. M. Crisci, Multifunctional TiO<sub>2</sub> coatings for cultural heritage, *Progress in Organic Coatings* 74 (1) (2012) 186–191.
- [50] M.E. David, R.-M. Ion, R.M. Grigorescu, L. Iancu, E.R. Andrei, Nanomaterials used in conservation and restoration of cultural heritage: an up-to-date overview, *Materials* 13 (2020) 2064.
- [51] P. Munafò, G.B. Goffredo, E. Quagliarini, TiO<sub>2</sub>-based nanocoatings for preserving architectural stone surfaces: an overview, *Construction and Building Materials* 84 (2015) 201–218.
- [52] H. Barberousse, B. Ruot, C. Yéprémian, G. Boulon, An assessment of façade coatings against colonisation by aerial algae and cyanobacteria, *Building and Environment* 42 (7) (2007) 2555–2561.
- [53] S.A. Ruffolo, F. De Leo, M. Ricca, A. Arcudi, C. Silvestri, L. Bruno, C. Urzi, M.F. La Russa, Medium-term in situ experiment by using organic biocides and titanium dioxide for the mitigation of microbial colonization on stone surfaces, *International Biodeterioration and Biodegradation* 123 (2017) 17–26.
- [54] S.A. Ruffolo, M. Ricca, A. Macchia, M.F. La Russa, Antifouling coatings for underwater archaeological stone materials, *Progress in Organic Coatings* 104 (1) (2017) 64–71.
- [55] N. Wiley, *Environmental Plant Physiology*, Garland Science, Taylor & Francis Group, New York and London, 2016 (320 pp).
- [56] C. Hallmann, L. Stannek, D. Fritzlär, D. Hause-Reitner, T. Friedl, M. Hoppert, Molecular diversity of phototrophic biofilms on building stone, *FEMS Microbiology Ecology* 84 (2013) 355–372.